Blur Image Classification based on Deep Learning

Rui Wang(Member, IEEE), Wei Li, Runnan Qin
Key Laboratory of Precision Opto-mechatronics Technology, Ministry of Education, School of Instrumentation Science and Opto-electronics Engineering
University of Beihang, Beijing, China
E-mail: wangr@buaa.edu.cn, liwei_beihang@buaa.edu.cn

JinZhong Wu
The Third Research Institute of China Electronics Technology Group Corporation
Beijing, China

***Abstract*—Blur type identification is significant for blind image recovery in image processing area. In this paper, an accurate classification system exploiting Convolution Neural Network (CNN) is designed to identify four blur types of images: defocus blur, Gaussian blur, haze blur and motion blur. A supervised learning model of Simplified-Fast-Alexnet (SFA), which is an abbreviated and modified version of Alexnet, is created to map the input images into a higher dimensional feature space, in which the blurs can be classified accurately. With proportional compressing the output number of each convolution layer in Alexnet by the ratio of 0.5 and removing the first two Full Connected layers (FCs) in Alexnet, the SFA successfully simplifies the Alexnet and overcomes the fatal disadvantage of parameter redundancy. Moreover, the batch normalization layers are added into the designated classifier to replace the dropout method, thus it can accelerate the convergence rate of deep network during the training stage by reducing internal covariate shift as well as alleviate the overfitting problem. Experiments demonstrate the remarkable performance of the suggested approach in comparison with the original Alexnet and the state-of-the-art on the frequently-used *Berkeley dataset* and *Pascal VOC 2007* dataset.**

Keywords—Blur image classification; image blur modeling; SFA model; batch normalization; deep covolution neural network

I. INTRODUCTION

Image blur type classification is significant to blur image restoration, meanwhile, it is a challenging problem because various factors can lead to image blurring. For instance, the interference of the natural fog (haze blur), optical lens distortion (defocus blur), the atmospheric turbulence (Gaussian blur), and the relative motion between camera and targets during exposure (motion blur) [1,2]. Those blur images are common in daily life, however, it is extremely hard to realize their automatic identification.

The methods for image blur identification are mainly divided into two groups: the handcrafted feature-based methods and the learned feature-based methods. Methods depend on handcrafted features need prior knowledge to extract the blur features which can differentiate the variety of blur images, then the selected features of sample images are applied to training the designate classifiers. However, the approaches based on the learned characteristics only demand the original blur images to learn the differences automatically among the different blur type images.

In Liu et al.'s work [3], several handcrafted blur features, for instance, local power spectrum slope and local autocorrelation congruency were utilized to train Bayes classifier, which realized the identification of the blur types. A similar method relying on the alpha channel blur feature has been presented by Su et al. [4], which had disparate circularity in terms of the extension of blurs. Gaussian blur, defocus blur and motion blur were classified by some discrimination functions and decision rules [5] based on blur features which were extracted from the twice FFT transform spectrum. The power spectrum feature-based SVM classifier in [6] was applied to both the artificially-distorted images and naturally-blurred images assessment. Though the above-mentioned methods can achieve the classification or evaluation of the blur images in a degree, however, the robustness of these classification methods are not very satisfactory for practical applications.

Recently, a lot of researchers have shifted their attention from the heuristic priori method to the learned deep architecture in order to accomplish a lot of vision tasks. From Jain et al.'s work [7], the superiority of Convolution Neural Network (CNN) in denoising the images polluted by Gaussian noise could be observed. Moreover, a simple single-layered neural network based on multi-valued neurons was reported by Aizenberg et al. to identify four blur types [8]: defocus blur, rectangular blur, motion blur and Gaussian blur. The most recently, another learned-based method exploited pre-trained deep neural network (DNN) was proposed by Ruomei Yan and Ling Shao [9] to classify the different blur types. In addition, from reference [10], CNN was applied to detecting smiles from one single image and the results confirmed the potential of CNN in smile detection task. The classical model of CNN i.e. Alexnet was employed for dealing with thousands of categories classification issue [11], and wined the championship in 2012 ImageNet classification competition. The above-mentioned methods are all required a suitable model parameter initialization and a large number of samples for parameter learning, which may lead to the enormous consumption of time to obtain a trained classifier. Nevertheless, the special image processing component such as GPU and TPU has been participated into accelerating the image computing speed, which decreases time consumption of model training to a large degree, moreover, the outstanding performance of classification accuracy of those learned-based methods cannot be neglected by most researchers.

Inspired by the successful cases [8,9] of blur type identification and the remarkable performance of Alexnet in image classification tasks [11], a supervised SFA architecture was proposed to achieve classifying the four blur types (haze blur, Gaussian blur, defocus blur and motion blur) accurately and effectively.

II. METHODOLOGY

A. Image Blur Modeling

Image blur issue can be regarded as the image degradation process from the high-quality images to the low-quality blurred images [12]:

$$F(\mathrm{x}) = h(\mathrm{x}) * f(\mathrm{x}) + n \tag{1}$$

where F denotes the degraded image, f is the lossless image, h remarks the blur kernel a.k.a. the point spread function (PSF), $*$ means the convolution operator, and n indicates the additional noise, here, n is the Gaussian white noise.

In many practical applications, such as remote sensing and satellite imaging, Gaussian kernel function was regarded as the kernel function of atmospheric turbulence, it is expressed as follows:

$$h(\mathrm{x},\sigma) = \frac{1}{\sqrt{2\pi}\sigma}\exp(-\frac{x_1^2 + x_2^2}{2\sigma^2}),\ \mathrm{x} \in R \tag{2}$$

In which, σ is the kernel radius, R is the support region usually met the 3 σ criteria [13].

Motion blur is another blur to be considered, which is caused by the relative linear motion between the target and camera [14], and the PSF is as follows:

$$h(\mathrm{x}) = \begin{cases} \frac{1}{M},\ (x_1, x_2)\begin{pmatrix}\sin(\omega)\\ \cos(\omega)\end{pmatrix} = 0,\ x_1^2 + x_2^2 \le \frac{M^2}{4} \\ 0,\ \text{otherwise} \end{cases} \tag{3}$$

where M denotes the length of motion in pixels and ω indicates the angle between motion direction and the x axis.

Defocus blur is the most common to be seen in daily life and it can be modeled by the cylinder function:

$$h(\mathrm{x}) = \begin{cases} \frac{1}{\pi r^2},\ \sqrt{x_1^2 + x_2^2} \le r^2 \\ 0,\ \text{otherwise} \end{cases} \tag{4}$$

where r demonstrates the blur radius which is proportional to the extent of defocus.

Haze blur is caused by the interference of natural fog. In this paper, haze blur is not simulated by any PSF, due to that enormous samples are existed in real life and easy to be collected for experiment applications.

B. Batch Normalization in SFA

As we all know, image normalization can accelerate computation speed during the training stage. The normalization layer in Alexnet a.k.a. local response normalization can be expressed as the formula (5).

$$x_{norm}^{(k)} = \frac{x^{(k)}}{1 + \sqrt[\beta]{\frac{\alpha}{n}\sum_i x_i^2}} \tag{5}$$

In which, n is the neighborhood size for regularization, α is the zoom factor, β is the exponent, $x^{(k)}$ is the k^{th} input pixel in the sample images and x_i is the pixels in the local response region.

However, according to reference [15], the batch normalization cannot only achieve the function of the local response normalization in formula (5), but also can tolerate the relative large learning rate during model training. In addition, the batch normalization can overcome the fatal disadvantage of overfitting problem. The basic principle of batch normalization is illustrated as follows:

$$\bar{X}_{norm}^{(k)} = \frac{X^{(k)} - E[X^{(k)}]}{\sqrt{Var[X^{(k)}] + \varepsilon}} \tag{6}$$

where $\bar{X}_{norm}^{(k)}$ is the k^{th} normalized output of the convolution layers, $X^{(k)}$ is the k^{th} original output of the convolution layers, $E[X^{(k)}]$ is the expectation over the batch input samples, and $Var[X^{(k)}]$ is the variance of the batch input samples, ε is a micro-constant.

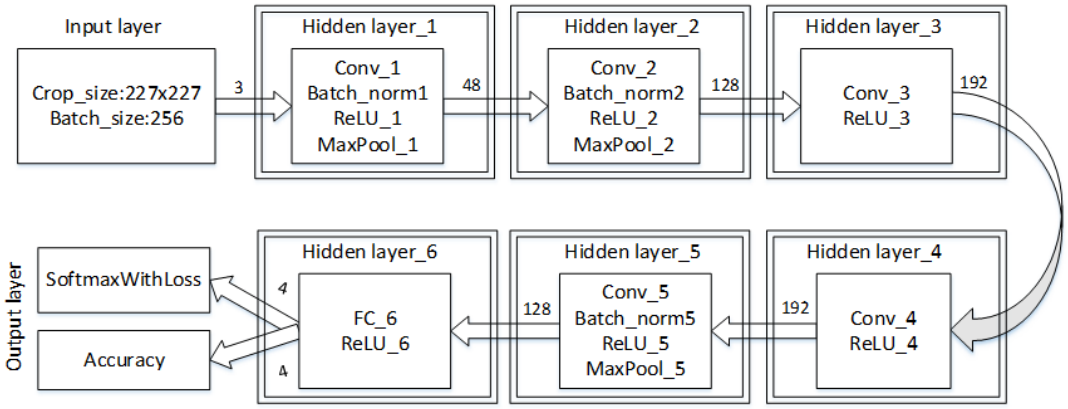

Fig.1. Overall architecture of SFA

As we all know, the nonlinear mapping function of sigmoid and tanh are easy to trapped into the gradient vanishing problem, and only the linear part can be employed for nonlinearity computing, hence the model expression ability is extremely restricted. In order to overcome this disadvantage, the output of batch normalization layer is modified as the formula (7).

$$y^{(k)} = \gamma^{(k)} \cdot \bar{X}_{norm}^{(k)} + \beta^{(k)} \tag{7}$$

where $\gamma^{(k)}$, $\beta^{(k)}$ are the pair-parameters for scaling and shifting the normalized value $\bar{X}_{norm}^{(k)}$, they are learned along with the remains model parameters during the whole training stage to enhance the representation ability of the designate network.

C. Overall Architecture of SFA

The overall architecture of SFA is shown in Fig.1, there are six hidden layers including five convolution layers and one full connected layer. SFA is a simplified-modified version of Alexnet. On the one hand, the output number of each convolution layer of Alexnet is proportional compressed by the ratio of 0.5. The reason for doing this is that, our four blur type classification is a relative simple task comparing the thousands of image categories in 2012 ImageNet classification competition. A complicated model may face the fatal disadvantage of parameter redundancy, hence, a relative simplified model should be generated for handling our specific issue. Moreover, the enormous time consumption for parameters learning decreases the performance of the classifier in consideration of speediness and real-time property, which is not favored in practical applications. On the other hand, the first two FCs are removed from the original model of Alexnet to enhance the speediness andreal-time performance because more than 80 percent parameters are stored in FCs. However, when the two FCs are removed, the dropout method disappeared at the same time, which may render the model confronting the serious overfitting problem. From Sec.II.*B*, the batch normalization not only can normalize the learned feature maps, but also can successfully resolve the overfitting problem. Therefore, the batch normalization is added in to the designate model.

From Fig.1, the size of the input images is 227×227×3. In the hidden layer 1, the first convolution layer(Conv 1) filters the inputs by the parameters: 48 kernels of size 11×11, stride of 4 pixels and pad of 0. Sequentially, the batch normalization layer normalizes the 55×55 learned feature maps which come from Conv 1. Thenceforth, ReLU 1 layer conducts the non-linearity computation on the output of batch normalization layer, and the Maxpool_1 layer compresses the optimized feature map with the parameters: kernel of size 3×3, stride of 2 pixels and pad of 0. Hence, the 48×27×27 feature maps are obtained as the output of the hidden layer_1.

The process of the received feature maps of hidden layer 2 and hidden layer 5 are similar with hidden layer 1. The parameters of the Conv 2 are: kernel of size 5×5, stride of 1 pixel and pad of 2 pixels; the MaxPool 2 with the parameters: kernel of size 3×3, stride of 1 pixel and pad of 0. Conv_5 layer with the parameters: kernel of size 3×3, stride of 1 pixel and pad of 1; parameters of MaxPool_5 layer is: kernel of size 3×3, stride of 2 pixels and pad of 0.

The hidden layer 3 and hidden layer 4 are without batch normalization and pooling layers, Conv 3 layer with parameters: kernel of size 5×5, stride of 1 pixel and pad of 2 pixels; the parameters of Conv 4 is: kernel of size 3×3, stride of 2 pixels and pad of 0. The hidden layer 6 just includes the ReLU 6 and FC 6. The data flow of the different hidden layers of SFA is as follows: 227×227×3→27×27×48→13×13×128→13×13×192→13×13×192→6×6×128→1×1×4 (from left to right respectively represent the input layer, hidden layer_1, ⋯, hidden layer_5 and FC_6 layer).

D. Details of SFA Training

After the whole architecture of SFA is constructed in Sec.II.*C*, the details of model training are illustrated in this section. The classical model training method of Stochastic Gradient Descent (SGD) is applied to training our designate model, with the parameters of batch_size 256, forgetting factor i.e. momentum 0.9, and weight decay 0.0003. Therefore, the update rule for weight w_i is as formula (8).

$$\begin{cases} v_{i+1} = \mu \cdot v_i - \lambda \cdot \nabla L(w_i) \\ w_{i+1} = w_i + v_{i+1} \end{cases} \tag{8}$$

where i is the iteration index, μ is the forgetting factor, v_{i+1} is the temporary variable, λ is the current learning rate, and $\nabla L(w_i)$ is average differential of weight w_i over the i^{th} batch.

Referring from Nair and Hinton [16], Rectified Linear Units (ReLUs) can achieve a faster training speed than the other units such as tanh with the same architecture and parameters, moreover, ReLUs can successfully overcome the Gradient Vanishing Problem during model training stage. The equation of ReLUs can be expressed as follows:

$$f(x) = \begin{cases} x, & x \geq 0 \\ 0, & x \leq 0 \end{cases} \tag{9}$$

where x is a linear combination of the weights and pixels of the target regions.

SoftmaxWithLoss is employed in calculating the loss value for guiding the model training. Firstly, compute the probabilities of that the input sample belongs to the corresponding classes by according the formula (10), thenceforth, calculate the loss value by referencing the equation (11).

$$P_i = \frac{e^{x_i - \bar{x}}}{\sum_j^K e^{x_i - \bar{x}}} \tag{10}$$

in which, K is the number of total classes, p_i is the probability of the sample belonging to the i^{th} category, $\bar{x}$ is the average value of the predicted result of FC_6 layer. The loss value is acquired by equation (11).

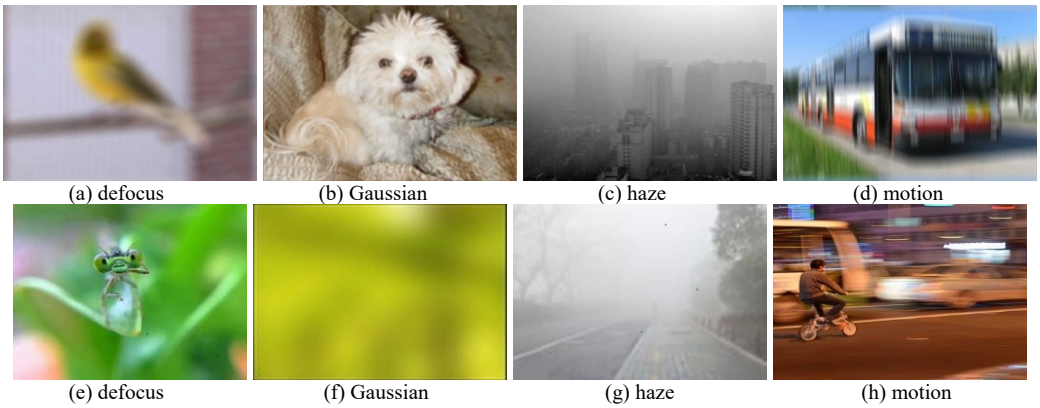

(a) defocus (b) Gaussian (c) haze (d) motion

(e) defocus (f) Gaussian (g) haze (h) motion

Fig.2. Sample images of simulated and natural blurred images. By the comparison of (a)(b) and (e) (f) in Fig.2, it can be observed that the defocus blur and Gaussian blur is difficult to distinguish by human eyes, however, from the experiment results, the trained SFA classifier can easily identify their differences.

$$Loss = -\log(p_t) \tag{11}$$

in formula (11), t is the truth label of the sample image. The output value of the loss layer is the average of the batch samples.

In addition, the weights of kernels are initialized by the Gaussian distribution with the parameters of zero-mean and standard deviation of 0.01, the biases is the constant of 0 or 1. Learning policy is step with the stepsize of 20000 and basic learning rate of 0.01. 200000 samples are implemented to train the SFA on the PC with NVIDIA-GTX-1080 8GB GPU.

III. Experiment Results And Analysis

A. Experimental Setup

Training dataset: The Oxford building dataset and Caltech 101 dataset are selected as our training set. 10000 images are chosen from the two datasets randomly, one-third are degraded by the Gaussian blur PSF with the kernel size of R in the range of [3,11] and the σ in the range of [1,10]; one-third are degraded by the motion blur PSF with the blur parameter M within the scope of [9,17] and ω within scope of [0°,180°]; the remains are degraded by the defocus blur PSF with the blur parameter r within the scope of [5,25]. The Gaussian white noise n with mean of [-2,2] and variance of [1,10]. Among the artificial blur images, half of them are partial blurred and the others are blurred over the whole image. 3300 natural blurred haze pictures are gathered from the famous domestic and foreign websites e.g. *Baidu.com, Flicker.com and Pabse.com*. The final training sample patches are cropped from the obtained blur images both including the whole and partial blurred images with the crop size of 128×128×3 and the stride of 64 pixels, the class labels are 0-defocus, 1-Gaussian, 2-haze, 3-motion. Finally, a training dataset consisting of 200000 global blur patches is acquired to train the designate classifier.

Testing dataset1: Berkeley dataset 200 images and Pascal VOC 2007 dataset are selected to be our testing dataset. In total 22240 global blur test sample patches are obtained by the same procedure of the training patches, in which 5560 haze blur image patches possess the same sources with training samples and the remains are proportional occupied by the other three classes.

Testing dataset2: In order to testify the practical performance of proposed classifier in real application, a dataset consisting of 10080 natural global blur image patches is constructed. The samples are all collected from the same websites as the haze blur samples in Training dataset. All the samples both of the training dataset and two testing datasets are uniformly distributed to enhance the generalization of the suggested classifier. Several sample images both the artificial blur and natural blur are shown in Fig.2.

B. Blur Image Classification Results and Analysis

The model parameters setting of SFA is according to the discussion in Sec.II.*D* and it is trained by the PC with the NVIDIA-GTX-1080 8GB GPU under the Caffe framework. The loss and accuracy curves are shown in Fig.3.

From Fig.3 (a)(b)(c), it can be learned that the shape of the curves is different due to the imparity of the stepsize of the learning policy. The abscissas denote the iterations and only 0-60000 are shown for a better visual effect. The criteria for finishing the model training is that the losses and the accuracy achieve their extremums and keep the relatively stable state. From (a)(b)(c), through the details of two model are different, both the losses and accuracy are reach the similar value, which indicates the performance of two models are equivalent in terms of the classification accuracy standard.

Visualization results of filter parameters and learned feature maps of each layer are illustrated in Fig.4. and Feature maps samples are shown in Fig.5. It can be observed from Fig.4.(a)(b) that after a long time training the smooth filter with no noise contamination, no important correlation and no structural mess can be gained, which indicates the model parameters are well learned. From Fig.5, (a) is the RGB three channels of the original sample image. (b)(c) are feature maps learned from the shallow layers of Conv_1 and Conv_2, where they reflect the global features such as the shape features and texture features. (d) is the feature map learned from the deep layers of Conv_5 which mirrors the local characteristics that are with low readability and difficult for understanding.

When the suggested classifiers are obtained, the filter parameters and the learned feature maps of each layer can be acquired. Weight maps samples are illustrated in Fig.4. Feature maps samples are shown in Fig.5.

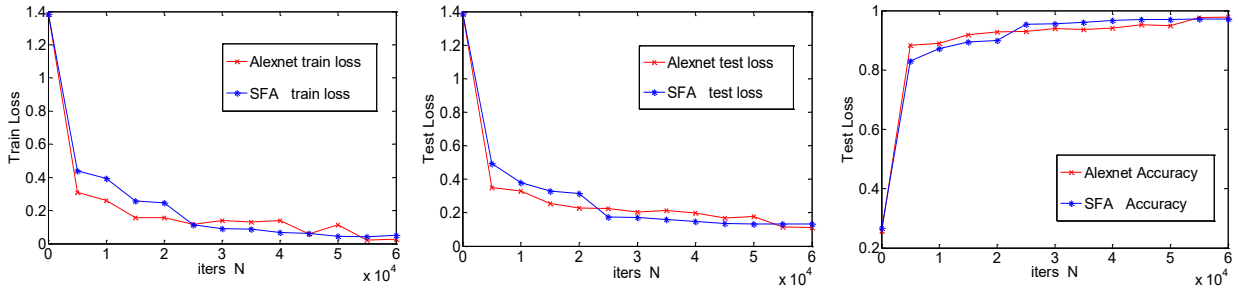

(a) Train loss curves (b) Test loss curves (c) Accuracy curves

Fig.3. Loss and Accuracy curves of Alexnet model and SAF model.

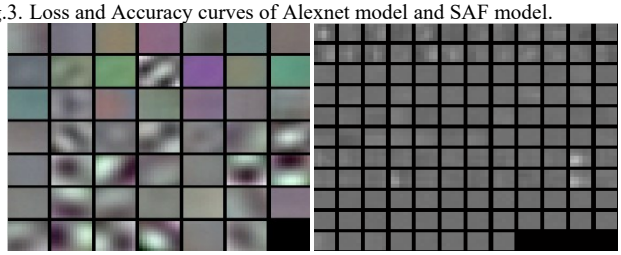

(a) (b)

Fig.4. Weights maps of Conv_1 layer and Conv_2 layer. (a) The 48 filters kernels of size 11×11×3 learned by the Conv_1 layer on the 227×227×3 input images; (b) The 128 convolution kernel of size 5×5×1 learned by the Conv_2 layer on the 27×27×3 feature of the Maxpool_1 layer.

It can be observed from Fig.4. (a)(b) that after a long time training the smooth filter with no noise contamination, no important correlation and no structural mess can be gained, which indicates the model parameters are well learned. From Fig.5, (a) is the RGB three channels of the original sample image. (b)(c) are feature maps learned from the shallow layers of Conv_1 and Conv_2, where they reflect the global features such as the shape features and texture features. (d) is the feature map learned from the deep layers of Conv_5 which mirrors the local characteristics that are with low readability and difficult for understanding.

On the one hand, performance comparison of SFA and Alexnet under several criteria and the results are illustrated in Table.1 where, P_N is the model parameter numbers, L_N is the model depth, F_T is forward propagation time of the single image, B_T is the error backward propagation time of a single image, CLF_T is the time of identify a single image, Tr_T is the model training time and Error is the classification error rate over the testing dataset1.

From the TABLE.I, it can be learned that the P_N of Alexnet is approximately 1000 times of SFA. the B_T is dramatically different on account of that model parameters demanding to be learned are great disparity. The CLF_T of SFA is 0.5s economy than Alexnet, which indicates the SFA is more suitable in practical applications. The total training time of SFA is less than one day, yet, the Alexnet requires about two days. Through, the classification error rate of SFA is 0.0105 greater than Alexnet, the short training time cost and the fast classification speed can cover its micro-shortage.

On the other hand, we also compare the proposed method with the state-of-the-art. The original architectures of Bayes classifier [3] and two-step way [4] achieved detecting the blur region first, and then classifying the obtained blur areas. However, in our algorithm, the blur detection was accomplished in the pre-processing stage and only the whole blurred patches are send to the classifier for identification. From our preliminary work [17], support vector machine(SVM) classifier based on the Gaussian radial basis function has successfully classified the ovarian cancer images, here, we also shown its blur image classification performance. Moreover, the common used classifier such as Softmax and Random Forest were chosen for comparison. In our implementation, Bayes [3], SVM [17], Softmax and Random Forest were all desigined with 35 handcrafted blur features such as statistic features, texture features and spectrum features, and then they were evaluated on our testing datasets. In addition, the single-layered NN[8] and DNN framework [9] based on learned features were selectd for comparision. The classification accuracy rate is employed in evaluating the performance, which is defined as equation (12).

$$Accuracy = \frac{N_{correct}}{N_{total}} \times 100\% \qquad (12)$$

where the $N_{correct}$ denotes the correct classified sample number, N_{total} indicates the total sample number required to be identified.

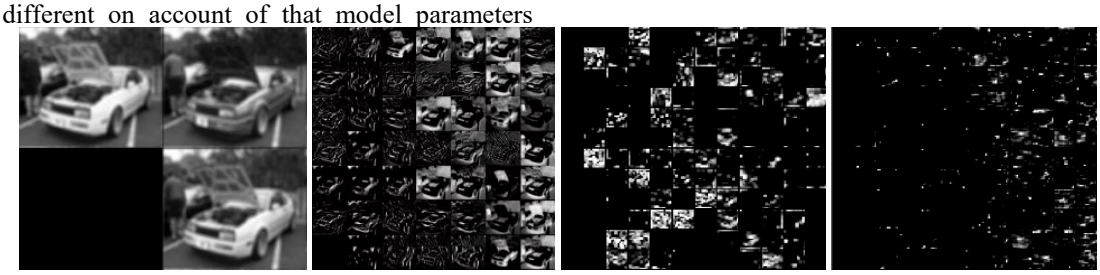

(a) (b) (c) (d)

Fig.5. Learned feature maps of different layers. (a) The RGB three channels of the input image;(b) The 55×55×48 feature maps of the Conv_1 layer; (c) the feature maps of MaxPool_2 with the size of 13×13×128 and (d) is the feature maps of Conv_5 layer with the size of 6×6×128

TABLE I. COMPARISON OF ALEXNET MODEL AND SFA MODEL.

Name	P_N	L_N	F_T	B_T	CLF_T	Tr_T	Error
Alexnet	58649189	7	0.28ms	0.56ms	0.578s	43h	2.26%
SFA	50489	5	0.27ms	0.27ms	0.078s	23.67h	3.21%

TABLE II. COMPARISON OF SFA CLASSIFIER AND THE STATE-OF THE -ART

Methods	Features	Accuracy1	Accuracy2
Two-step way[4]	Handcrafted	88.78%	
***Bayes*[3]**		70.07%	54.16%
***SVM* [17]**		*82.73%*	*80.22%*
Softmax		*75.68%*	*72.64%*
Random Forest		*83.46%*	*75.41%*
Single-layered NN[8]	learned	94%-97%	
DNN[9]		95.2%	
Alexnet		*97.74%*	*94.10%*
SFA		*96.99%*	*93.75%*

The comparison results are demonstrated in the Table 2. Need to be cleared that the classification accuracies of two-step way [4], single-layered NN [8] and DNN [9] are come from the original articles, the data of the other methods are testified on our datasets. Accuracy1 is test on the testing dataset1 and Accuracy2 is test on the testing dataset2. Single-layered NN [8] shows the single class classification accuracy and the remained methods demonstrate the total classes classification accuracy.

It can be observed from Table.2 that the prediction accuracy (>90%) of learned feature-based methods is generally superior to the ones (<90%) whose features are handcrafted. The classification accuracy of SFA on simulated testing dataset is 96.99%, which is slightly lower than Alexnet of 97.74%, nevertheless, it is still better than DNN model of 95.2%. In addition, the best performance of SFA on natural fuzzy datasets is 93.75%, slightly lower than that of 94.10%, however, the data in Table.1 has shown the speediness and real-time performance of SFA is significantly better than Alexnet. Therefore, we believe that SFA is better qualified for blur image classification tasks.

IV. CONCLUSION

In this article, a convolution neural network (CNN) of Simplified-Fast-Alexnet(SFA) based on the learning features is proposed for handling the classification issue of defocus blur, Gaussian blur, haze blur and motion blur four blur type images. SFA, Alexnet and others blur classification methods are testified with our own simulated blur dataset and natural blur dataset respectively. The experiment results demonstrate that the performance of classification accuracy of SFA, which is 96.99% for simulated blur dataset and 92.75% for natural blur dataset, is equivalent to Alexnet and superior to other classification methods. In addition, the model training time of 23h and single image classification time of 0.078s for SFA apparently outperform the Alexnet. Therefore, the SFA possesses the strong competitiveness than other classification methods in dealing with the blur image classification task. On the other hand, it is found in our experiment that the size of the learned feature maps and the input image have significant influence on the classification results, hence, exploring the pre-processing method of the input image to improve the performance of the classifier is our future research direction.

ACKNOWLEDGEMENTS

This work was supported in part by a grant from National Natural Science Foundation of China (61673039).

REFERENCES

[1] Elder, J.H., Zucker, S.W.: 'Local scale control for edge detection and blur estimation', IEEE Transactions on Pattern Analysis and Machine Intelligence, 1998, 20, (7), pp. 699–716

[2] Wang, R., Li, R., Sun, H.: 'Haze removal based on multiple scattering model with superpixel algorithm', Signal Processing, 2016, 127, (C), pp. 24–36

[3] Liu, R., Li, Z., Jia, J. 'Image partial blur detection and classification'. In: Computer Vision and Pattern Recognition, 2008. CVPR 2008. IEEE Conference on. (, 2008.pp. 1–8

[4] Su, B., Lu, S., Tan, C.L. 'Blurred image region detection and classification'. In: International Conference on Multimedea 2011, Scottsdale, Az, Usa, November 28- December. (, 2011. pp. 1397–1400

[5] Bi, X.J., Wang, T. 'Adaptive blind image restoration algorithm of degraded image'. In: Image and Signal Processing, 2008. CISP '08. Congress on. (, 2008. pp. 536–540

[6] Mavridaki, E., Mezaris, V.: 'No-reference blur assessment in natural images using fourier transform and spatial pyramids', 2015, pp. 566–570

[7] Jain, V., Seung, H.S. 'Natural image denoising with convolutional networks'. In: Conference on Neural Information Processing Systems, Vancouver, British Columbia, Canada, December. (, 2008. pp. 769–776

[8] Butakoff, C., Karnaukhov, V.N.: 'Blurred image restoration using the type of blur and blur parameter identification on the neural network', Proceedings of SPIE-The International Society for Optical Engineering, 2002, 4667, pp. 460–471

[9] Yan, R., Shao, L.: 'Blind image blur estimation via deep learning', IEEE Transactions on Image Processing, 2016, 25, (4), pp. 1910–1921

[10] Bianco, S., Celona, L., Schettini, R.: 'Robust smile detection using convolutional neural networks', Journal of Electronic Imaging, 2016, 25, (6), pp. 063002

[11] Krizhevsky, A., Sutskever, I., Hinton, G.E. 'Imagenet classification with deep convolutional neural networks'. In: International Conference on Neural Information Processing Systems. (, 2012. pp. 1097–1105

[12] Molina, R., Mateos, J., Katsaggelos, A.K.: 'Blind deconvolution using a variational approach to parameter, image, and blur estimation', IEEE Transactions on Image Processing, 2006, 15, (12), pp. 3715–27

[13] Chen, F., Ma, J.: 'An empirical identification method of gaussian blur parameter for image deblurring', IEEE Transactions on Signal Processing, 2009, 57, (7), pp. 2467–2478

[14] Kundur, D., Hatzinakos, D.: 'Blind image deconvolution', IEEE Signal Processing Magazine, 2002, 13, (3), pp. 43–64

[15] Ioffe, S., Szegedy, C.: 'Batch normalization: Accelerating deep network training by reducing internal covariate shift', Computer Science, 2015,

[16] Nair, V., Hinton, G.E. 'Rectified linear units improve restricted boltzmann machines'. In: International Conference on Machine Learning. (, 2010. pp. 807–814

[17] Wang, R., Li, R., Lei, Y., Zhu, Q.: 'Tuning to optimize svm approach for assisting ovarian cancer diagnosis with photoacoustic imaging.', Bio-medical materials and engineering, 2015, 26, (s1), pp. S975 – S981